Stellar Populations in the Milky Way and Beyond
Proceedings IAU Symposium No. 395, 2026
J. Meléndez, C. Chiappini, R. Schiavon & M. Trevisan, eds.
doi:10.1017/S1743921325000742

Applicability of elemental abundance ratios as age indicators in evolved stars

Gražina Tautvaišienė, Erika Pakštienė, Arnas Drazdauskas, Yuriy Chorniy, Vilius Bagdonas, Carlos Viscasillas Vázquez, Šarūnas Mikolaitis, Renata Minkevičiūtė, Edita Stonkutė and Markus Ambrosch

Institute of Theoretical Physics and Astronomy, Vilnius University, Sauletekio av. 3, 10257, Vilnius, Lithuania
email: grazina.tautvaisiene@tfai.vu.lt

Abstract. A unique opportunity to use the TESS Space Mission data for the asteroseismic age determination, the Gaia Space Mission data for more precise stellar birthplace determinations, and detailed chemical composition studies allow us to take further steps in Galactic chemical evolution studies. In this contribution, we address the stellar age determination which has by now relatively large uncertainties. Calibrations of [C/N] with respect to age are investigated on the basis of a sample of Galactic field stars with asteroseismic ages determined using the TESS Space Mission data. For the first time, it was investigated how the stellar evolutionary stage influences the age determination from [C/N] abundance ratios which are sensitive to mixing in stellar atmospheres. The availability of asteroseismic stellar ages allowed us to address in more detail the emerging chemical-clock method applicability for stars of the thin and thick discs at different Galactic radial distances.

Keywords. Galaxy: evolution, stars: age, asteroseismology, stars: low-mass

1. Introduction

Age is a stellar quantity that cannot be directly measured, and one must rely on other physical characteristics of the star that are correlated with age to derive it. Progress depends largely on what observational data and theoretical models are available. Firstly, there were discussions of whether the colour of a star indicates its age (Pierson 1890), could stars be as old as $10^{13} - 10^{14}$ years, and how one has to account for the existence of uranium and thorium (Lindemann 1925). Attempts to evaluate the age of globular clusters using their colour-magnitude diagrams were extensively applied and, for example, yielded about $6.5 \cdot 10^9$ years age for M 3 (Haselgrove & Hoyle 1956) compared to the later evaluation of $11.39 \cdot 10^9$ years (Forbes & Bridges 2010). Stellar rotation, magnetic activity, and lithium abundance were also considered as promising indicators of age (Hazlehurst & Thomas 1970; Wilson & Wooley 1970; Skumanich 1972). A review of the applicability of chemical elements for stellar age indication was provided by Pagel (1972), who outlined nitrogen as the most promising chemical element. For further developments in the field, see, e.g. Larsson-Leander (1972); Cowan *et al.* (1991); Mamajek (2009); Soderblom (2010); Kurtz (2022) and references therein. The need for reliable stellar ages has always existed. In this presentation, some recent and our current work is presented in a rather new direction of stellar age determinations using so-called chemical clocks.

© The Author(s), 2026. Published by Cambridge University Press on behalf of The International Astronomical Union. This is an Open Access article, distributed under the terms of the Creative Commons Attribution licence (https://creativecommons.org/licenses/by/4.0/), which permits unrestricted re-use, distribution and reproduction, provided the original article is properly cited.

https://doi.org/10.1017/S1743921325000742 Published online by Cambridge University Press

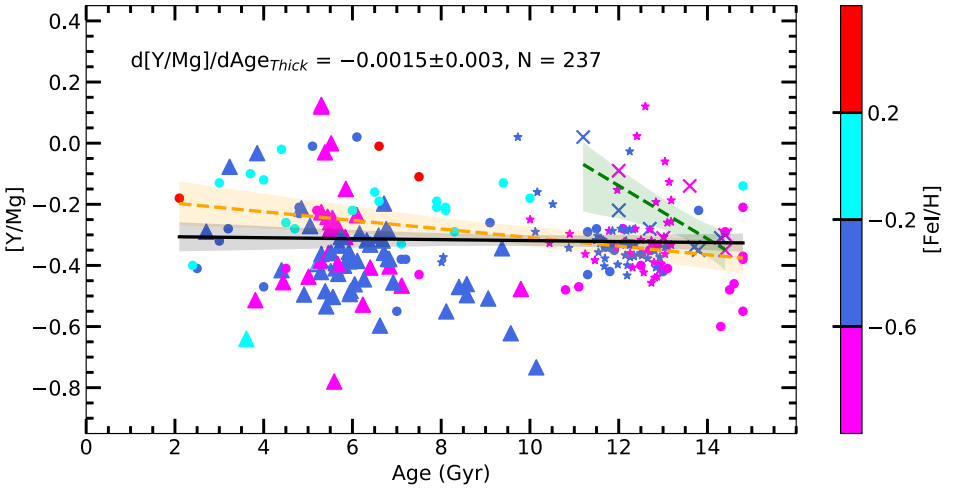

Figure 1. [Y/Mg] of the thick-disc stars colour-coded by metallicity as a function of age. Stars investigated by Tautvaišienė et al. (2021) are marked by triangles, and are supplemented by data from Bensby et al. (2014) (dots), Delgado Mena et al. (2017) and Adibekyan et al. (2012) (stars), and Titarenko et al. (2019) (crosses). The black continuous line is a fit to the entire sample of 237 stars. For a comparison, the dashed green line represents the trend taken from Titarenko et al. (2019), who computed it for the AMBRE sample of 11 thick-disc stars; and the dashed yellow line represents the trend that we computed using Bensby et al. (2014) data alone covering the entire investigated age interval. The shadowed areas show the 95% confidence interval for the ordinary least-squares regressions. The figure is taken from Tautvaišienė et al. (2021).

2. [Y/Mg] ratio as age indicator

A key motivating paper was that of Nissen (2015), who used HARPS spectra with a resolution of 115 000 and S/N≥ 600 of 21 solar twin stars in the solar neighbourhood and the Sun to determine very precise ($\sigma \sim 0.01$ dex) differential abundances of elements and investigated how well element abundance ratios correlate with stellar age. A clear correlation with the reduced chi-square of the fit equal to $\chi^2 = 0.71$ was received for [Y/Mg] and age. Later studies revealed that the relations between ages and abundance ratios obtained from samples of stars located in a limited region of the Galaxy cannot be translated into general relations valid for the whole disc (Casali 2020; Magrini et al. 2021; Tautvaišienė et al. 2021; Viscasillas Vázquez et al. 2022), and most importantly to the thick disc of the Galaxy (Tautvaišienė et al. 2021).

According to Tautvaišienė et al. (2021), the correlation of the [Y/Mg] ratio with age in the thick disc of the Galaxy is negligible. They collected determinations of [Y/Mg] and ages for a sample of 237 thick-disc stars: 76 they took from their study, 66 stars from Bensby et al. (2014), 88 stars from Delgado Mena et al. (2017) and Adibekyan et al. (2012), and 11 stars from Titarenko et al. (2019). In Figure 1, we present a plot taken from Tautvaišienė et al. (2021) that shows a flat relationship of [Y/Mg] with age.

For the field stars, ages can be determined most accurately from asteroseismic pulsations. The NASA Transiting Exoplanet Survey Satellite (TESS) space telescope (Ricker et al. 2015) not only plays a very important role in the search of exoplanets around bright stars, but also provides stellar asteroseismic variability data. In our ongoing study, we decided to try to determine asteroseismic ages for a sample of 1250 bright stars located within the TESS Continuous Viewing Zone and 12 deg around it. For these stars, Y and Mg were determined in our previous studies (Tautvaišienė et al. 2020, 2022)

https://doi.org/10.1017/S1743921325000742 Published online by Cambridge University Press

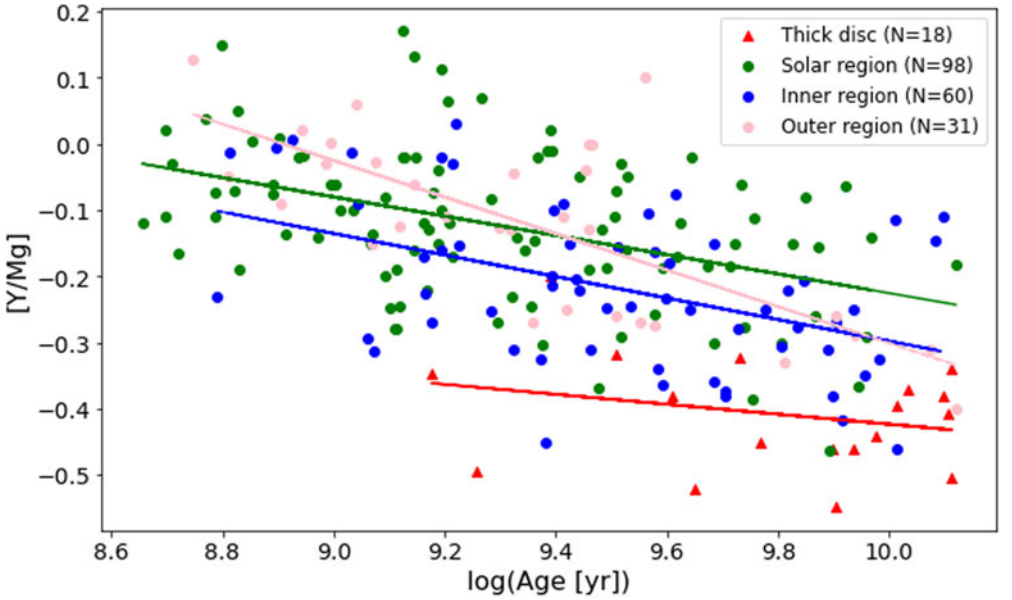

Figure 2. [Y/Mg] versus asteroseismic stellar age for thin- and thick-disc stars. The thin-disc stars are marked according to their mean galactocentric distances (the blue dots are for stars with $R_{\rm mean} < 7.5$ kpc, the green dots for $7.5 \leq R_{\rm mean} \leq 8.5$ kpc, and the pink dots are for $R_{\rm mean} > 8.5$ kpc. The red triangles represent the thick-disc stars. The lines correspond to [Y/Mg] versus age relations for the listed groups of stars.

and the current study, carried out using the high-resolution spectrograph and 1.65 m telescope at the Moletai Astronomical Observatory in Lithuania.

In Figure 2, the [Y/Mg] and age relation is displayed for 207 stars with the asteroseismic ages determined from the reliable pulsations and [Y/Mg] determinations for the thin- and thick-disc stars. The thin disc stars are divided according to their mean radial distances, $R_{\rm mean}$, in the Galaxy. The stars with $R_{\rm mean} < 7.5$ kpc, with $7.5 \leq R_{\rm mean} \leq 8.5$ kpc, and with $R_{\rm mean} > 8.5$ kpc. It is seen that the [Y/Mg] relation with age depends on the mean galactocentric distance, whereas stars of the thick disc, despite the fact that the sample is quite small, confirm negligible correlation.

For the asteroseismic age determination, we analysed 60-minute and 2-minute cadence TESS light curves of our set of stars observed in the sectors 13–26. The light curves, flattened and cleaned of outliers, were processed using the Lightkurve package Lightkurve Collaboration (2018). This enabled us to obtain the pulsation spectra of the stars and determine asteroseismic parameters such as the frequency at maximum power, $\nu_{\rm max}$, and the large frequency separation, $\Delta\nu$, assuming that all stars in our sample may be solar-type pulsators. Only stars exhibiting clear solar-like pulsations with easily recognisable ridges of $\ell = 0$, 1, and 2 modes in Echelle diagrams were selected for further analysis and age determination.

Using $\nu_{\rm max}$, $\Delta\nu$, the spectroscopic effective temperature and metallicity, we calculated stellar mass, radius, surface gravity, and luminosity based on the classical scaling relations Kjeldsen & Bedding (1995).

We then used the online PARAM interface (v.1.5) for the Bayesian estimation of the stellar parameters (Da Silva et al. 2006; Rodrigues et al. 2014, 2017). To account for the mass loss in our calculations, we applied the Reimers mass-loss efficiency coefficient $\eta_R = 0.4$. This value well reflects the average value of the Reimers coefficient considering different empirical contexts and models (McDonald & Zijlstra 2015; Valle et al. 2018).

https://doi.org/10.1017/S1743921325000742 Published online by Cambridge University Press

Recently, Brogaard et al. (2024) showed that mass loss cannot be accurately described by a Reimers mass-loss law with a single value of η_R, however. This should encourage further development of the theory that underlies the processes involved in mass loss.

The ages were determined using a grid of the MESA isochrones (Rodrigues et al. 2017), where individual radial-mode frequencies and large separations $\Delta\nu$ were calculated for each model on the grid. As the PARAM description states that the MESA isochrones are available in the mass range $0.6 \leq M < 2.5\ M_{\odot}$, for stars with a scaling relation mass greater than 2.5 $M_{\odot}$ (up to 4 $M_{\odot}$), the age was calculated with the PARSEC isochrones (Bressan et al. 2012) instead. Finally, a two-step Bayesian method (Rodrigues et al. 2014) was used to determine the ages of the investigated stars.

3. [C/N] ratio as age indicator

Elemental abundances of carbon and nitrogen in red giants are sensitive to stellar characteristics, including mass and age. Theoretical predictions on how [C/N] changes with stellar age have been presented in many studies, for example, by Salaris et al. (2015) and Lagarde et al. (2017, 2019).

(Casali et al. 2019) provided an empirical relationship between stellar ages and [C/N] using open star clusters, observed by the *Gaia*-ESO and APOGEE surveys, as calibrators. Masseron & Gilmore (2015) accomplished a comprehensive analysis of [C/N] ratios using APOGEE data for stars in the thin and thick discs of the Galaxy. Larger [C/N] ratios in thick-disc stars than in thin-disc stars at the same metallicity confirmed their older age. They concluded that current stellar evolution models cannot reproduce the observed C/N ratios for thick disc stars.

Having in mind that low-mass giants experience not only the first dredge-up at the base of the red giant branch (RGB), but also the extra-mixing at the RGB luminosity bump (Lagarde et al. 2019, and references therein), it is necessary to take into account changes of [C/N] ratios caused by these evolutionary processes while elaborating calibrations with age.

Having at hand the high-resolution [C/N] determinations (Tautvaišienė et al. 2020, 2022) and the stellar age determined as described in the previous section, we started to investigate whether the same [C/N] versus age calibration can be used for the age determination of giants in the evolutionary phase below the RGB luminosity bump (we will call these stars RGB BB), where the extra-mixing starts, for stars above the RGB bump (RGB AB), and for stars in the helium-core burning phase (RC). Separating stars into these evolutionary phases is not an easy task. Nowadays, asteroseismic data can also be attracted for this task.

At later stages of stellar evolution, such as the red giant branch and helium core-burning phases (the red clump (RC) in the case of our sample), g-modes originating in the deep stellar interior begin to influence surface p-modes through mode coupling, creating detectable mixed modes splitted into a distinct pattern of mixed modes.

Bedding et al. (2011) demonstrated that g-modes lead to period spacing, a characteristic separation between consecutive oscillation periods of splitted $\ell = 1$ modes. This coupling is particularly sensitive to the core structure, allowing the period spacing to reflect differences in burning processes, such as the hydrogen shell burning on the RGB and helium-core burning in RC stars. These effects become increasingly prominent as structural changes in the core of a star and its envelope amplify the interaction between these two modes, making them valuable indicators of the stellar evolutionary stage (Bedding et al. 2011; Mosser et al. 2012).

For the identification of stellar evolutionary stages, we adopted the methodology developed by Bedding et al. (2011). However, the evolutionary stage was classified only for 31 RGB and for 50 RC stars using this method. For the classification of the remaining stars,

https://doi.org/10.1017/S1743921325000742 Published online by Cambridge University Press

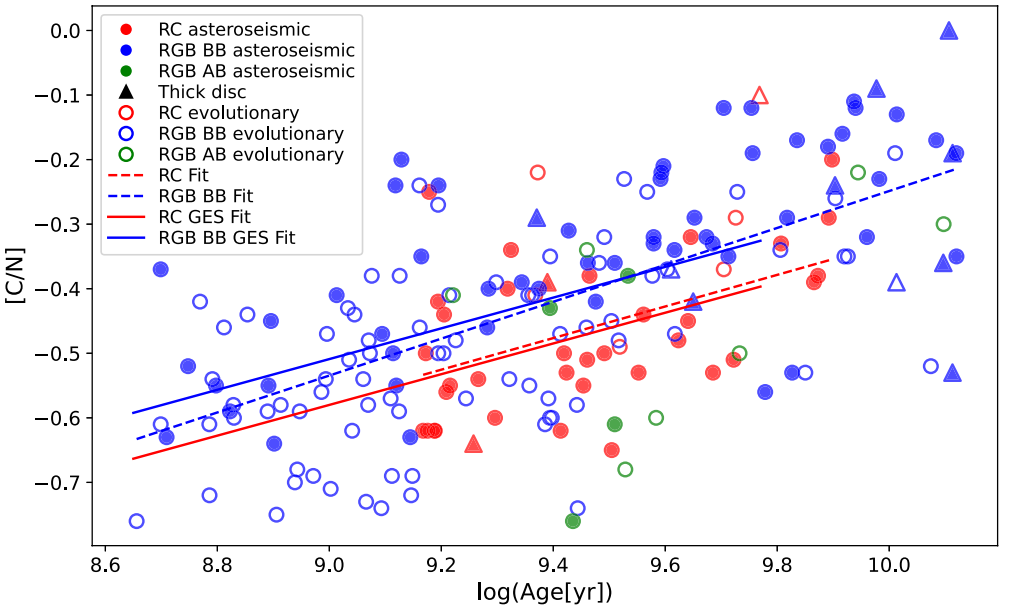

Figure 3. [C/N] versus asteroseismic stellar age. The dots mark stars for which the evolutionary stage was identified using the asteroseismic methods. The open circles are for stars identified using the evolutionary methods. The red symbols are for the He-core burning red clump stars, the blue symbols for the RGB stars below the luminosity bump, whereas the green symbols mark RGB stars above the luminosity bump. The thick-disc stars are shown by triangles. The continuous and dashed lines represent [C/N] versus age fits for the *Gaia*-ESO open clusters and for the field stars in the thin disc, respectively.

their location relative to the evolutionary tracks by Bressan et al. (2012) was considered. Also we investigated for which stars the mass loss affects the stellar age determination. For RC stars and RGB stars above the RGB luminosity bump (RGB AB), the mass loss is larger than in RGB stars below the luminosity bump (RGB BB) Origlia et al. (2002). This evaluation also allowed us to assess the evolutionary stages of the remaining stars.

Figure 3 demonstrates the [C/N] dependency on asteroseismic stellar ages for stars at different evolutionary stages in the thin and thick discs of the Galaxy. The dependencies of the investigated field stars are compared with the dependencies computed for a sample of open clusters, which we currently investigate using the *Gaia*-ESO survey data. In the Gaia-ESO survey (Gilmore et al. 2022; Randich et al. 2022), C and N abundance determinations are present for 45 clusters. The 18 clusters have stars in several evolutionary phases, below and above the RGB luminosity bump and in the clump.

The robustness of stellar evolutionary stage identification and the age determination for open clusters is rather high; therefore, a good agreement of the field stars fits with the fits of open clusters (Figure 3) is much appreciated. The sample of the thick-disc star is quite small; however, it seems that there is no obvious systematic difference compared to locations of the thin-disc stars.

The influence of stellar and cluster location in the Galaxy was not taken into account in these fits (Figure 3). In Figure 4, like in the case of [Y/Mg], the thin-disc RGB stars located below the RGB luminosity bump, the largest group in our sample, were divided according to their mean radial distances, $R_{\rm mean}$. The stars with $R_{\rm mean} < 7.5$ kpc, with $7.5 \leq R_{\rm mean} \leq 8.5$ kpc, and with $R_{\rm mean} > 8.5$ kpc are plotted with the corresponding trends of [C/N] versus the asteroseismic age. It is seen that the [C/N] relation versus age

https://doi.org/10.1017/S1743921325000742 Published online by Cambridge University Press

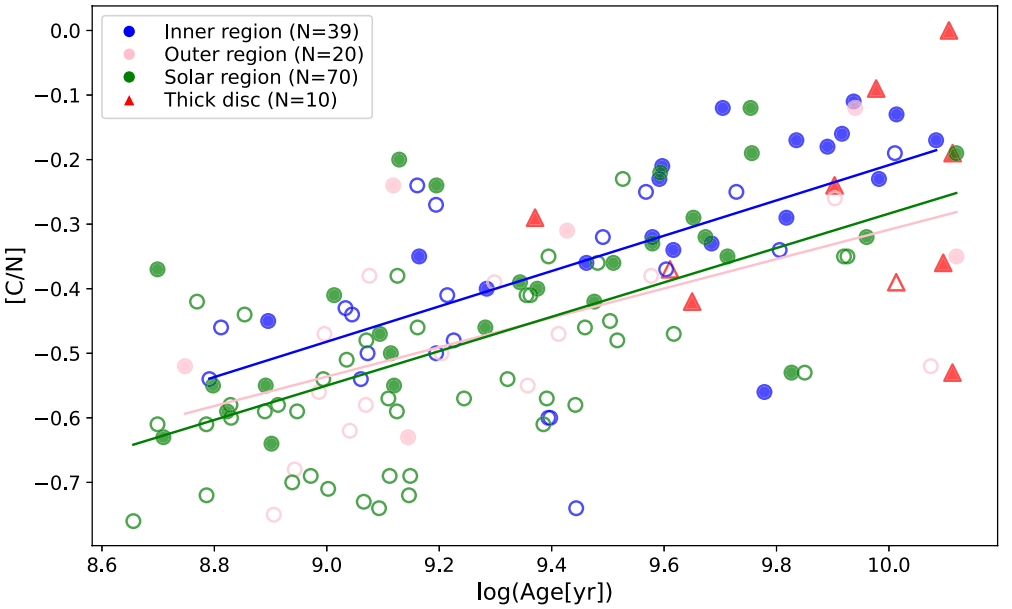

Figure 4. [C/N] versus asteroseismic stellar age for thin- and thick-disc red giant branch stars located below the RGB luminosity bump. The thin-disc stars are marked according to their mean galactocentric distances (the blue dots are for stars with $R_{\rm mean} < 7.5$ kpc, the green dots for $7.5 \leq R_{\rm mean} \leq 8.5$ kpc, and the pink dots are for $R_{\rm mean} > 8.5$ kpc. The red triangles represent the thick-disc stars. The filled and open symbols indicate the method of evolutionary stage determination. The lines correspond to [C/N] versus age relations for the listed groups of stars.

slightly depends on the mean galactocentric distance. The available thick-disc RGB BB stars are also displayed, but are too few for this kind of investigation.

4. Concluding remarks

The precision of stellar age determination is continuously increasing. The ESA Kepler and NASA TESS space telescopes, which provided data of asteroseismic stellar pulsations, gave a big boost to progress in this field. Unfortunately, asteroseismic pulsations cannot be robustly detected in all stars. For example, in a sample of 1250 low-mass giant stars, located within the TESS Continuous Viewing Zone and 12 deg around it and observed the largest number of times, the asteroseismic ages were determined just for 20% of them in our study. However, such asteroseismic age determinations are very valuable for calibrations of other age indicators like chemical element ratios. However, in order to have accurate chemical clocks, the precision of element abundance determinations has to be enhanced, and many factors like stellar location in the Galaxy and its evolutionary stage have to be taken into account.

Acknowledgements

We thank the financial support of the Research Council of Lithuania (LMTLT grant No. P-MIP-23-24). We also thank Beatriz Barbuy for being a role-scientist for all of us.

References

Adibekyan, V. Z., Sousa, S. G., Santos, N. C., *et al.* 2012, *A&A*, 545, A32
Bedding, T. R., Mosser, B., Huber, D., *et al.* 2011, *Nature*, 471, 608
Bensby, T., Feltzing, S., & Oey, M. S. 2014, *A&A*, 562, A71

https://doi.org/10.1017/S1743921325000742 Published online by Cambridge University Press

Bressan, A., Marigo, P., Girardi, L., Salasnich, B., Dal Cero, C., Rubele S., Nanni A. 2012, *MNRAS*, 427, 127
Brogaard, K., Miglio, A., van Rossem, W. E., Willett, E., Thomsen, J. S. 2024, *A&A*, 691, A288
Casali, G., Magrini, L., Tognelli, E., *et al.* 2019, *A&A*, 629, A62
Casali, G., Spina, L., Magrini, L., *et al.* 2020, *A&A*, 639, A127
Cowan, J. J. & Thielemann, F.-K., and Truran, J. W. 1991, *ARA&A*, 29, 447
da Silva, L., Girardi, L., Pasquini, L., *et al.* 2006, *A&A*, 458, 609
Delgado Mena, E., Tsantaki, M., Adibekyan, V. Z., *et al.* 2017, *A&A*, 606, A94
Forbes, D. A. & Bridges, T. 2010, *MNRAS*, 404, 1203
Gilmore, G., Randich, S., Worley, C. C., *et al.* 2022, *A&A*, 666, A120
Haselgrove, C. B. & Hoyle, F. 1956, *MNRAS*, 116, 527
Hazlehurst, J. & Thomas, H.-C. 1970, *MNRAS*, 150, 311
Kjeldsen H., Bedding T. R. 1995, *A&A*, 293, 87
Kurtz, D. 2022, *ARA&A*, 60, 31
Lagarde, N., Robin, A. C., Reylé, C., and Nasello, G. 2017, *A&A*, 601, A27
Lagarde, N., Reylé, C., Robin, A. C., *et al.* 2019, *A&A*, 621, A24
Larsson-Leander, G. 1972, in IAU Colloq. 17: Age des Etoiles, p.2
Lightkurve Collaboration *et al.* 2018, Lightkurve: Kepler and TESS time series analysis in Python, Astrophysics Source Code Library (ascl:1812.013)
Lindemann, F. 1925, *Nature*, 115, 229
Magrini, L., Vescovi, D., Casali, G., *et al.* 2021, *A&A*, 646, L2
Mamajek, E. E. 2009. In The Ages of Stars, Proc. IAU Symp. 258, ed. E. E. Mamajek, D. R. Soderblom, R. F. G. Wyse. Cambridge, Cambridge Univ. Press, p. 375
Masseron, T., Gilmore, G. 2015, *MNRAS*, 453, 1855
McDonald I., Zijlstra A. A. 2015, *MNRAS*, 448, 502
Mosser, B., Goupil, M. J., Belkacem, K., *et al.* 2012, *A&A*, 540, A143
Nissen, P. E. 2015, *A&A*, 579, id.A52
Origlia, L., Ferraro, F. R., Fusi Pecci, F., Rood, R. T. 2002, *ApJ*, 571, 458
Pagel, B. E. J. 1972, in IAU Colloq. 17: Age des Etoiles, p.47
Pierson, W. M. 1890, *PASP*, 2, 105
Randich, S., Gilmore, G., Magrini, L., *et al.* 2022, *A&A*, 666, A121
Ricker, G. R., Winn, J. N., Vanderspek, R., *et al.* 2015, *JATIS*, 1, 014003
Rodrigues T. S., *et al.* 2014, *MNRAS*, 445, 2758
Rodrigues T. S., *et al.* 2017, *MNRAS*, 467, 1433
Salaris, M., Pietrinferni, A., Piersimoni, A. M., Cassisi, S. 2015, *A&A*, 583, A87
Skumanich, A. 1972, *ApJ*, 171, 565
Soderblom, D. R. 2010, *ARA&A*, 48, 581
Tautvaišienė, G., Mikolaitis, Š., Drazdauskas, A., *et al.* 2020, *ApJS*, 248, 19
Tautvaišienė, G., Viscasillas Vázquez, C., Mikolaitis, Š., *et al.* 2021, *A&A*, 649, A126
Tautvaišienė, G., Mikolaitis, Š., Drazdauskas, A., *et al.* 2022, *ApJS*, 259, 45
Titarenko, A., Recio-Blanco, A., de Laverny, P., Hayden, M., and Guiglion, G. 2019, *A&A*, 622, A59
Valle, G., Dell'Omodarme, M., Prada Moroni, P. G., Degl'Innocenti, S. 2018, *A&A*, 609, A58
Viscasillas Vázquez, C., Magrini, L., Casali, G., *et al.* 2022, *A&A*, 660, A135
Wilson, O. & Woolley, R. 1970, *MNRAS*, 148, 463

https://doi.org/10.1017/S1743921325000742 Published online by Cambridge University Press